JOURNAL OF THEORETICAL
AND APPLIED MECHANICS
40, 4, pp. 825-846, Warsaw 2002

ON THE MAGNETIZATION-BASED LAGRANGIAN METHODS FOR 2D AND 3D VISCOUS FLOWS. PART 2 – NUMERICAL IMPLEMENTATION AND RESULTS

Piotr Duszyński
Piotr Olszewski
Marta Poćwierz
Andrzej Styczek
Jacek Szumbarski

Institute of Aeronautics and Applied Mechanics, Warsaw University of Technology
e-mail: jasz@meil.pw.edu.pl

The numerical implementation of the Lagrangian method using particles of the magnetization field (magnetons) has been considered. A detailed description of essential elements of the algorithm has been provided. The presentation has focused on computations of stretching, where a novel integral-based rather than point wise approach has been proposed. The results of test computations, carried out for viscous flows past 2D and 3D bodies, have been presented. Difficulties with obtaining stable large-time simulations have been encountered and discussed. It has also been shown that, in contrast to flows around solid bodies, the vortex dynamics in the absence of boundaries can be successfully simulated, however, some consistent remeshing technique may be necessary to achieve appropriate resolution.

Key words: viscous flow, Navier-Stokes equations, magnetization, stretching

1. Introduction

In the first part of the paper (Styczek and Szumbarski, 2002), the theoretical foundations of the magnetization-based Lagrangian method for 2D and 3D flows have been presented. This Part is devoted to the description of the numerical implementation of this method.

One of the crucial elements of the method is the treatment of the stretching. It terms of the magneton discretization, the stretching is responsible

for modification in time of individual "charges" of magnetization particles. The rule governing this modification should be derived from the equation of evolution of the magnetization field, but there is no unique way to do that. Originally, Buttke (Buttke and Chorin, 1993) proposed computing the stretching term in a point-wise manner (in a center of each magneton). That method can work well only when the magnetons are very small and the spatial variation of the stretching term on the length-scale of the magneton core is negligible. These requirrements, however, are not likely to be satisfied, at least not in the whole flow domain. Actually, in some parts of the flow domain the stretching term exhibits rapid space variation. Typical examples are a region near the body surface (like the boundary layer) as well as "active" regions of the wake behind the body, i.e. regions with highly concentrated vorticity. In order to account for the spatial structure of the stretching in such extreme cases, we develop an alternative method based on local averaging of the stretching. This approach proved to be more suitable than the point wise treatment.

The properties of the proposed numerical method are tested in a series of sample computations. We run numerical simulation of fluid motion in domains with and without solid boundaries: the flow past a circular contour in 2D, the flow past a spherical body in 3D and the flow induced by a vortex-like structure evolving in the 3D space.

2. Particles of magnetization (magnetons) and their motion

Consider an external flow around a smooth contour (2D) or a closed surface (3D). The magnetization field $\boldsymbol{m} = \boldsymbol{m}(t, \boldsymbol{r})$ is, in general, defined in the whole flow domain. It has been shown in Part 1 of the paper that the corresponding (induced) velocity field can be expressed by the following formulae

$$\boldsymbol{u} = \boldsymbol{m} - \nabla\phi = (Id - \nabla\Delta^{-1})\boldsymbol{m} = \mathcal{P}\boldsymbol{m} \tag{2.1}$$

The operator $\mathcal{P}$ is called the Hodge projector. The inverse of the Laplace operator Δ^{-1} can be easily evaluated when no boundary conditions are imposed. Consider a single magneton embedded in an unbounded fluid. Assuming isotropy of the inner structure of the magneton one can write

$$\boldsymbol{m}(t, \boldsymbol{r}) = \boldsymbol{m}_0(t) g(|\boldsymbol{r} - \boldsymbol{r}_0(t)|) \tag{2.2}$$

where the core function g vanishes identically outside the magnetons interior, i.e. when $|\boldsymbol{r} - \boldsymbol{r}_0(t)| \geqslant a$. Here, the symbol a denotes the radius of the spherical

core of the magneton and $\boldsymbol{r}_0(t)$ describes an instantaneous location of the magneton center. The core function g is assumed smooth and it determines the velocity induced by the magneton. This velocity can be calculated from formulae derived in Part 1 and re-written below as

$$\boldsymbol{u} = \boldsymbol{m}_0(t)[g(r) - F(r)] - \frac{(\boldsymbol{m}_0 \cdot \boldsymbol{r})\boldsymbol{r}}{r^2}[g(r) - N_D F(r)] \tag{2.3}$$

where

$$F(r) = \frac{1}{r^{N_D}} \int_0^r \xi^{N_D - 1} g(\xi)\, d\xi \tag{2.4}$$

and $N_D = 2$ or $N_D = 3$ for two or three-dimensional motion, respectively.

The value $F(a)$ defines the "charge" of the magneton, namely

$$Q = a^{N_D} F(a) \tag{2.5}$$

It is not difficult to show (see Part 1) that the velocity field induced outside the magneton core is potential accordingly to the formula

$$\boldsymbol{u} = -Q\nabla \frac{\boldsymbol{m}_0 \cdot \boldsymbol{r}}{r^{N_D}} \tag{2.6}$$

and that the spherical boundary of the core $r = a$ moves due to self-induction with the velocity

$$\boldsymbol{U} = (N_D - 1)\frac{Q}{a^{N_D}}\boldsymbol{m}_0 \tag{2.7}$$

Consider a magneton embedded in an ambient fluid moving with the velocity $\boldsymbol{v}$. We assume that the magneton's instantaneous velocity is the sum of the self-induced velocity $\boldsymbol{U}$ and the velocity of advection $\boldsymbol{v}$. In general, the advection is due to induction from other magnetons and additional constant vector field $\boldsymbol{V}_0$, introduced in order to ensure appropriate conditions at infinity. Thus, the formulae for complete velocity field at the center of the magneton can be written as follows

$$\boldsymbol{V}\Big|_{O_i} = \boldsymbol{U}_i + \sum_{k \neq i} \boldsymbol{u}(|\boldsymbol{r}_{O_i} - \boldsymbol{r}_{O_k}|) + \boldsymbol{V}_0 \tag{2.8}$$

The core function g can be chosen as a polynomial defined in the interval $[0, a]$ and expanded around zero for $r > a$. Such an expansion has to preserve appropriate regularity of the core function. Consequently, we obtain the magneton with a finite core as described above. The example is

$$g(r) = \left(\frac{r}{a}\right)^2 - \frac{8}{5}\frac{r}{a} + \frac{3}{5}$$

The admissible alternative is to construct the magneton with a infinite but spatially localized core. It can be achieved by choosing the following core function

$$g(r) = \mathrm{e}^{-\beta r^3} \qquad \beta > 0 \tag{2.9}$$

The constant β defines the core concentration in the sense that higher values of β yield more localized distributions of the magnetization. Roughly speaking, this constant plays the role of a^{-3} in the case of the finite core.

3. Simulation of viscosity by random walks

The magnetization field $\boldsymbol{m}$ is constructed as the sum of a large number of the magnetons. Each of them moves with accordance to an instantaneous velocity given by formula (2.8), and additionally performs a random walk. The random displacements of a magneton in consecutive time instants are statistically independent, and so are the random motions of different magnetons. The stochastic part of the magneton motion is to simulate the diffusion of the magnetization due to fluid viscosity. As it was described in Part 1, the location of the ith magneton center $\boldsymbol{r}_{O_i}$ stems from the following Itô differential equation

$$d\boldsymbol{r}_{O_i} = \boldsymbol{V}\Big|_{O_i} dt + \sqrt{2\nu}\, d\boldsymbol{W}_i \tag{3.1}$$

The symbol $d\boldsymbol{W}_i = [dW_{i,x}, dW_{i,y}, dW_{i,z}]$ denotes an infinitesimal increment of the vector Wienner process, whose scalar components are statistically independent. Since the diffusion coefficient $\sqrt{2\nu}$ is constant, equation (3.1) can be interpreted in the sense of Stratonovich (see Gardiner, 1990), and integrated using standard methods.

Equations (3.1) govern the motion of all magnetons in the flow domain. Looking at the flow field at a certain time instant, one can divide all magnetons into two categories: the "old" magnetons, i.e. the magnetons that were created in the past and are still present in the flow domain, and "new" magnetons, i.e. those currently being created. The satisfaction of the boundary conditions requires that new magnetons be continuously injected into the flow domain. It seems physically plausible to add them in the close vicinity of a surface of an immersed body. I should be noted that, due to a random walk and/or the self-induction, a magneton is able to move through the body surface into its interior. If such an event occurs, the magneton can be simply removed from the simulation or it can be reflected back to the flow domain. Since the boundary

conditions are formulated for the velocity, both methods seem to be admissible, and the results of numerical computations should not be method-dependent. We will discuss this problem later.

4. The stretching effect

The stretching effect is described by the "source" term in the governing equation

$$\partial_t \boldsymbol{m} + (\boldsymbol{V} \cdot \nabla)\boldsymbol{m} = \nu \Delta \boldsymbol{m} + \underbrace{\begin{cases} -(\nabla \boldsymbol{V})^\top \boldsymbol{m} \\ (\boldsymbol{m} \cdot \nabla)\nabla \phi \end{cases}}_{\text{stretching term}} \tag{4.1}$$

The stretching term can assume one of two forms, as indicated in (4.1), depending on the choice of the gauge transform (see Part 1 for details).

As it has been explained in Part 1, the Lie-Trotter formula is used to separate the time-step advancing of the magnetization field into three consecutive parts. In the last stage, the magnetization is modified due to the source (or stretching) term appearing in the right-hand side of equation (4.1). Both variants of the stretching lead to a set of differential equations in the following form

$$\partial_t m^\alpha = B_{\alpha\beta} m^\beta \tag{4.2}$$

Dependently on the chosen variant of the stretching, the matrix $\mathbf{B}$ is defined by the first- order derivatives of the velocity $\boldsymbol{V}$ or by the second-order derivatives of the gauge potential φ

$$B_{\alpha\beta} = \begin{cases} -\partial_{x_\alpha} v^\beta \\ \partial_{x_\alpha x_\beta} \phi \end{cases} \tag{4.3}$$

Re-writing equation (4.2) in the matrix/vector form

$$\partial_t \boldsymbol{m} = \mathbf{B}\boldsymbol{m} \tag{4.4}$$

we see that the magnetization field evolves in time at a rate given by the action of the tensor field $\mathbf{B}$ on the "immersed" vector field. Considering a given instant of time, we can compute an average of the stretching action of $\mathbf{B}$ over one magneton

$$\frac{d\boldsymbol{m}_0}{dt} = \mathbf{B}^0 \boldsymbol{m}_0 \tag{4.5}$$

The averaged value $\mathbf{B}^0$ is given by the following integral

$$B^0_{\alpha\beta} = \frac{1}{4\pi Q}\int \left\{ \begin{array}{c} -\partial_{x_\alpha} v^\beta \\ \partial_{x_\alpha x_\beta}\phi \end{array} \right\} g(r)\, d\Omega \tag{4.6}$$

Integrating by parts, we obtain

$$B^0_{\alpha\beta} = \frac{1}{4\pi Q}\int \left\{ \begin{array}{c} v^\beta \\ -\partial_{x_\beta}\phi \end{array} \right\} \frac{dg(r)}{dr}\frac{x_\alpha}{r}\, d\Omega \tag{4.7}$$

Again, upper and lower expressions appearing in brackets in (4.6) and (4.7) refer to different variants of the stretching term.

The "upper" variant does not give any self-stretching, i.e. the averaged effect of the stretching of a single magneton on its own magnetization field is zero. This fact is due to formula (2.3) and the form of the integrand in (4.7). It can be noticed that the product $v^\beta x_\alpha$ is an anti-symmetric function and the integration over any spherical domain yields zero.

Formula (4.5) describes the instantaneous rate of time variation of the vector $\boldsymbol{m}_0$. Clearly, the change affects both the length of $\boldsymbol{m}_0$ and its direction in space. It is possible to consider these two effects separately.

Let m_0 denotes the length of the vector $\boldsymbol{m}_0$. The direction of $\boldsymbol{m}_0$ is described by the unitary vector $\boldsymbol{e} = \boldsymbol{m}_0/m_0$. Thus, we have $\boldsymbol{m}_0 = m_0\boldsymbol{e}$, equation (4.5) can be written as

$$\boldsymbol{e}\frac{dm_0}{dt} + m_0\frac{d\boldsymbol{e}}{dt} = m_0\mathbf{B}^0\boldsymbol{e} \tag{4.8}$$

and

$$\frac{1}{m_0}\frac{dm_0}{dt} = \langle \boldsymbol{e}, \mathbf{B}^0\boldsymbol{e}\rangle \qquad \frac{d\boldsymbol{e}}{dt} = \mathbf{B}^0\boldsymbol{e} - \langle \boldsymbol{e}, \mathbf{B}^0\boldsymbol{e}\rangle\boldsymbol{e} = (\boldsymbol{e}\times\mathbf{B}^0\boldsymbol{e})\times\boldsymbol{e} \tag{4.9}$$

Equation $(4.9)_1$ describes "pure stretching", i.e., describes time variation of the length of the vector $\boldsymbol{m}_0$. Equations $(4.9)_2$ governs, in turn, variation of the space direction of $\boldsymbol{m}_0$ or, equivalently, it describes pure rotation of $\boldsymbol{m}_0$.

According to $(4.9)_2$, an instantaneous angular velocity of the rotation of the vector $\boldsymbol{e}$ is $\boldsymbol{\vartheta} = \boldsymbol{e}\times\mathbf{B}^0\boldsymbol{e}$. Clearly, $\boldsymbol{\vartheta}$ is perpendicular to $\boldsymbol{e}$. It means that the three following unitary vectors

$$\boldsymbol{\ell}_1 = \boldsymbol{e} \qquad \boldsymbol{\ell}_2 = \frac{\boldsymbol{\vartheta}\times\boldsymbol{e}}{\|\boldsymbol{\vartheta}\times\boldsymbol{e}\|} \qquad \boldsymbol{\ell}_3 = \frac{\boldsymbol{\vartheta}}{\vartheta}$$

form the local Cartesian basis. Hence, the vector $\boldsymbol{e}$ can be expressed as

$$\boldsymbol{e} = \xi_1\boldsymbol{\ell}_1 + \xi_2\boldsymbol{\ell}_2 \tag{4.10}$$

and then the vector product $\boldsymbol{\vartheta} \times \boldsymbol{e}$ can be calculated

$$\boldsymbol{\vartheta} \times \boldsymbol{e} = \begin{vmatrix} \boldsymbol{\ell}_1 & \boldsymbol{\ell}_2 & \boldsymbol{\ell}_3 \\ 0 & 0 & \vartheta \\ \xi_1 & \xi_2 & 0 \end{vmatrix} = -(\vartheta\xi_2)\boldsymbol{\ell}_1 + (\vartheta\xi_1)\boldsymbol{\ell}_2 \tag{4.11}$$

Differentiating (4.10) and comparing with (4.11), we obtain ordinary differential equations for the functions $\xi_1(t)$ and $\xi_2(t)$

$$\frac{d\xi_1}{dt} = -\vartheta\xi_2 \qquad \frac{d\xi_2}{dt} = \vartheta\xi_1 \tag{4.12}$$

supplemented by appropriate initial conditions, i.e. $\xi_1(0) = 1$ and $\xi_2(0) = 0$. The first-order accurate integration yields

$$\xi_1(\Delta t) = \cos(\vartheta\Delta t) \qquad \xi_2(\Delta t) = \sin(\vartheta\Delta t)$$

which means that

$$\boldsymbol{e}(t+\Delta t) = \boldsymbol{e}(t)\cos(\vartheta(t)\Delta t) + \frac{\boldsymbol{\vartheta}(t) \times \boldsymbol{e}(t)}{\|\boldsymbol{\vartheta}(t) \times \boldsymbol{e}(t)\|}\sin(\vartheta(t)\Delta t) \tag{4.13}$$

The same order integration applied to differential equation $(4.9)_1$ gives

$$m_0(t+\Delta t) = m_0(t)\exp\Big(\langle \boldsymbol{e}, \mathbf{B}^0\boldsymbol{e}\rangle \Delta t\Big) \tag{4.14}$$

The procedure described above requires the matrix $\mathbf{B}^0$ to be found. The averaging of $\mathbf{B}$ consists in determination of nine scalar integrals, which have to be evaluated numerically. In general, an appropriate Gaussian quadrature is recommended. In the case of magnetons with unbounded cores, the Gaussian-Hermite integration method would be preferable.

5. The boundary conditions

It has been already mentioned that continuous generation of "new" magnetons in the vicinity of the body surface is necessary in order to satisfy the non-slip boundary condition imposed on the velocity field. At any time instant, the velocity can be expressed as a sum of three components: the velocity induced by the magnetons created in all previous steps of the flow simulation, the velocity induced by magnetons being currently created (yet unknown) and

the velocity of the uniform stream $\boldsymbol{U}_\infty$. If the no-slip condition is enforced in a point-wise manner, the following set of equations can be derived (see Part 1 of this paper, formula (5.5)), $i = 1, .., M$

$$\sum_{k=1}^{M} \boldsymbol{m}_{0k}^{n} \mathfrak{U}(|\boldsymbol{r}_{A_i} - \boldsymbol{r}_k^n|)\boldsymbol{e}_\alpha\Big|_{A_i} = -\boldsymbol{U}_\infty \boldsymbol{e}_\alpha\Big|_{A_i} - \sum_{(k)} \boldsymbol{m}_{0k}^{o}(|\boldsymbol{r}_{A_i} - \boldsymbol{r}_k^o|)\boldsymbol{e}_\alpha\Big|_{A_i} \tag{5.1}$$

The meanings of the symbols used in (5.1) are as follows:

- $\boldsymbol{m}_{0k}^{n}$ – magnetization charges of newly created magnetons
- $\boldsymbol{m}_{0k}^{o}$ – magnetization charges of already existing magnetons
- $\mathfrak{U}$ – induction operator (see expression (3.6) in Part 1)
- $\boldsymbol{r}_k^n$ – locations of the centers of newly created magnetons
- $\boldsymbol{r}_k^o$ – current locations of the centers of already existing magnetons
- $\boldsymbol{r}_{A_i}$ – locations of the collocation points at the surface of the immersed body
- $\boldsymbol{e}_\alpha\big|_{A_i}$ – local Cartesian basis at a collocation point A_i ($\alpha = 1, 2, 3$)
- $\boldsymbol{U}_\infty$ – velocity of the uniform stream at infinity.

It should be emphasized that the right-hand sides of system (5.1) involve only known values. In order to obtain a solvable problem, M collocation points at the surface have to be chosen. This way, system (5.1) will contain $3M$ equations with the same number of unknowns. As it was mentioned in the Part 1, the boundary conditions can be also formulated in an integral-mean rather that collocation manner. The numerical tests show that in such a case the resulting vectors $\boldsymbol{m}_{0k}^{n}$ ($k = 1, 2, .., M$) differ only slightly from those obtained from system (5.1).

During a numerical simulation, some magnetons will unavoidably cross the material surface and penetrate the interior of the body. Such events occur most likely for the magnetons located near the body surface. Theoretically, the only way a magneton can jump into the body interior is due to self-induction or due to diffusion modeled by a random walk. The possibility of the latter event decays rapidly with increasing distance from the surface, especially for flows with a low viscosity. In practice, the condition for the velocity at the boundary is not ideally fulfilled, and the time integration scheme is of a finite order. This is why a magneton can cross the body surface also due to the advectional part of its motion.

It should be clear that the boundary condition for the velocity is enforced at the beginning of each time step of the flow simulation. Having all magnetons moved to their new locations, this condition is violated. Then, another

generation of new magnetons appears in the vicinity of the surface, modifying the velocity field so that it satisfies the boundary condition again. The important issue is that this re-creation of the proper velocity distribution takes place independently of the method, removal or reflection, which has been used to deal with the magnetons, which left the flow domain in the previous time step. Using the local basis defined above, one can conclude that at the body surface the following condition is satisfied

$$\boldsymbol{n} \cdot \boldsymbol{\omega} = \boldsymbol{n} \cdot \operatorname{rot} \boldsymbol{u} = 0 \tag{5.2}$$

i.e., the vorticity vector at the surface has only a tangent component. Here, the symbol $\boldsymbol{n}$ denotes the unitary vector normal to the surface. Consider a magneton placed near the surface at the distance smaller than the radius of its core. Let S_m denote the portion of the surface embedded in the magneton core. Using formulae (2.1) and (2.2), one can verify that the vorticity flux through S_m equals zero, i.e.

$$\int\limits_{S_m} \boldsymbol{n} \cdot \boldsymbol{\omega} \, dS = \oint\limits_{\partial S_m} \boldsymbol{m} \cdot d\boldsymbol{\ell} = 0 \tag{5.3}$$

In the above, we use the fact that the magnetization vanishes at the boundary of the core. The meaning of equality (5.3) is following: although condition (5.2) cannot be imposed at each point of the surface, it is satisfied in an integral sense by individual magnetons.

6. Discussion of numerical results

In this Section, we discuss some numerical results obtained with the magnetization method. At the beginning of each time step, the magnetization charges of newly born magnetons are computed from equations (5.1). Next, all magnetons perform convective and diffusive (random) displacements accordingly to Itô's differential equations (3.1). Finally, the charges of the magnetons are modified due to the stretching effect as described in Section 4 (see Eq. (4.14)).

6.1. Simulation of a 2D flow past a circular contour

In this section, we discuss results of numerical simulations of two-dimensional viscous flow past a circular contour. The computations were car-

ried out with the use of magnetons with finite cores $(r = a)$ and polynomial core functions in the following form

$$g_1(r) = 2\frac{r^3}{a^3} - 3\frac{r^2}{a^2} + 1$$
$$g_2(r) = -9\frac{r^4}{a^4} + 20\frac{r^3}{a^3} - 12\frac{r^2}{a^2} + 1 \tag{6.1}$$

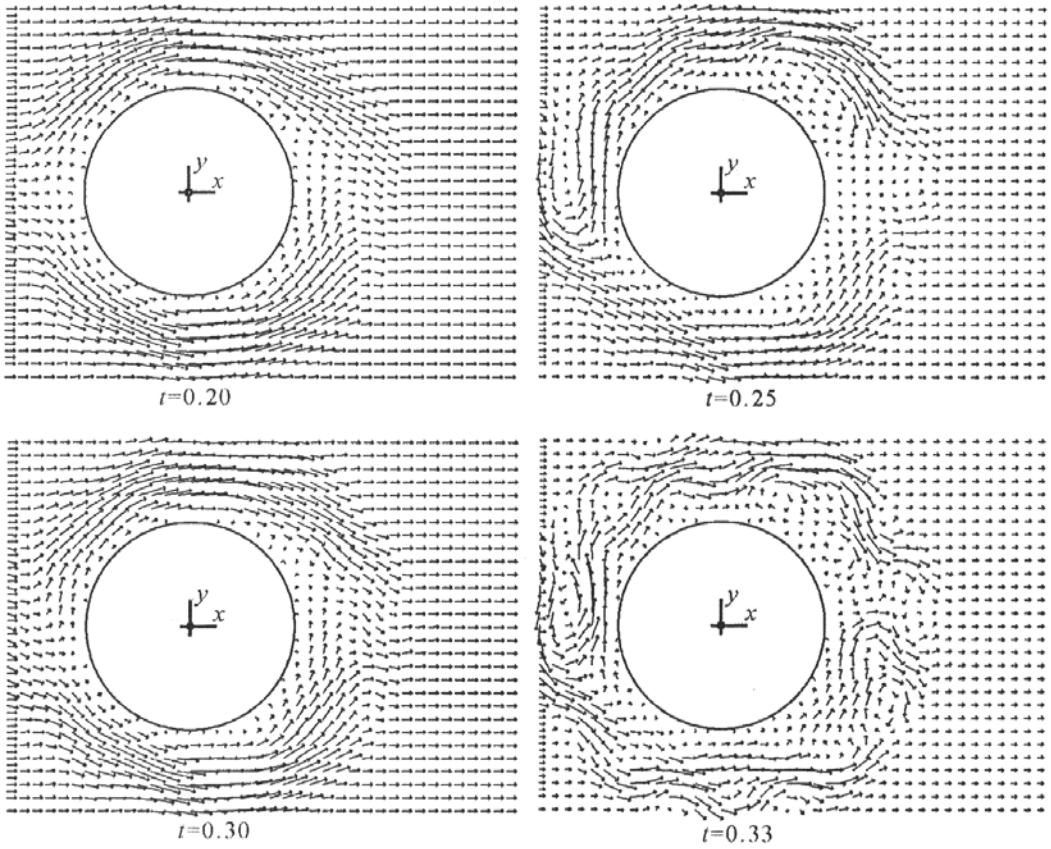

Fig. 1. Instantaneous velocity field computed for Re=100 (magnetons with the polynomial core function $g_2(r)$, Adams-Bashforth 3rd order integration scheme with $\Delta t = 0.01$)

Note that the core function $g_1(r)$ defines the magneton with a nonzero charge Q, while the function $g_2(r)$ corresponds to the magneton with $Q = 0$. The Adams-Bashforth third-order integration scheme (AB3) was used, and the influence of the magnitude of the time step Δt was tested. In Fig. 1, we present instantaneous velocity patterns for the flow with the Reynolds number Re=100, obtained with $\Delta t = 0.01$ and the core function g_2. Fig. 2 shows the

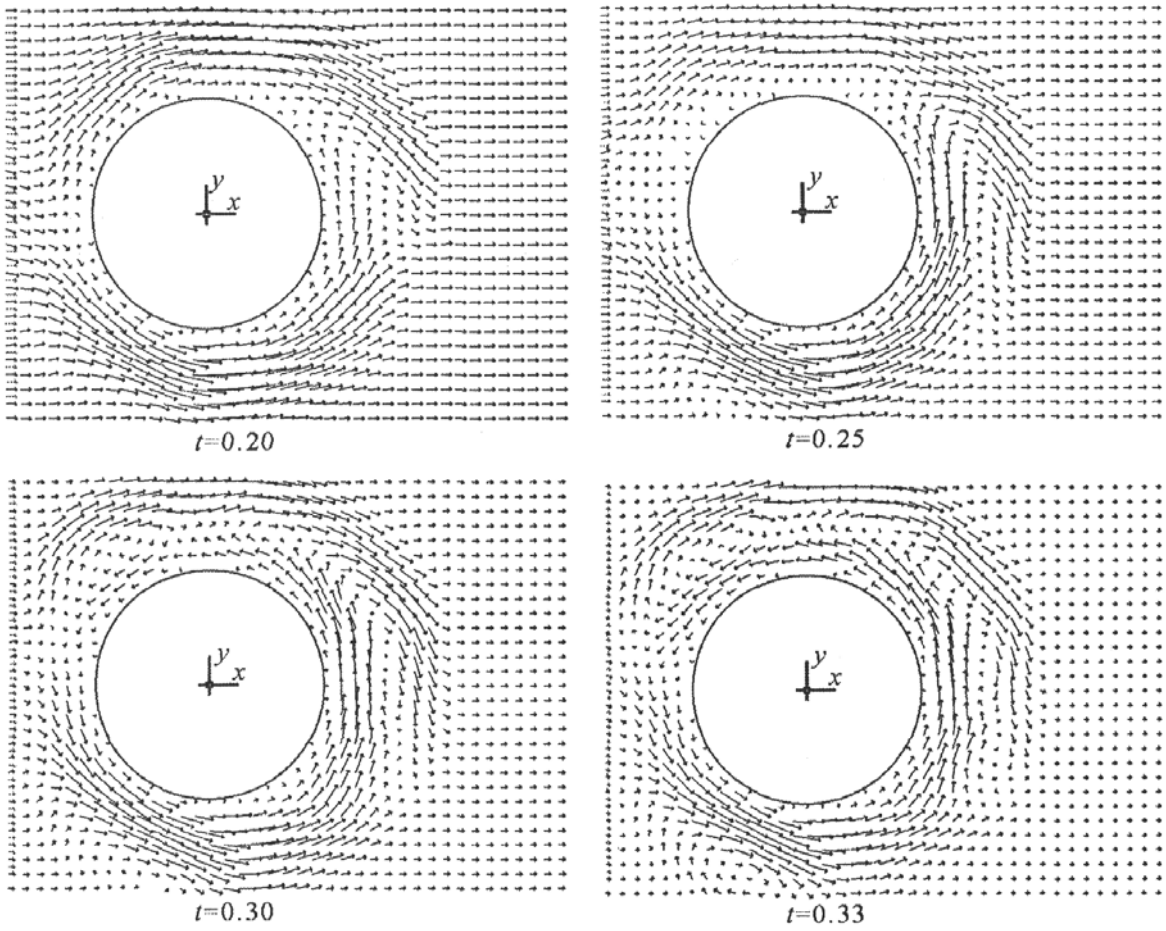

Fig. 2. Instantaneous velocity field computed for Re=100 (magnetons with the polynomial core function $g_2(r)$, Adams-Bashforth 3rd order integration scheme with $\Delta t = 0.00025$)

same case computed with a smaller time step ($\Delta t = 0.0025$). Analogous results for a higher Reynolds number Re=200 are shown in Fig. 3.

In order to assess the influence of an integration scheme, all above cases were computed with the fourth-order Runge-Kutta (RK4) method. The patterns of the velocity field obtained for Re=200 and the time step $\Delta t = 0.005$ are presented in Fig. 4.

The presented results show that that the numerical simulations did not give physically correct flow patterns. The boundary distributions of the magnetization were calculated properly, i.e. they ensured cancellation of the velocity at collocation points of the contour at each time step. The characteristic feature of the wake structure behind the cylinder contour (at considered values of the Reynolds number) contains a "chain" of large vortices with alternating

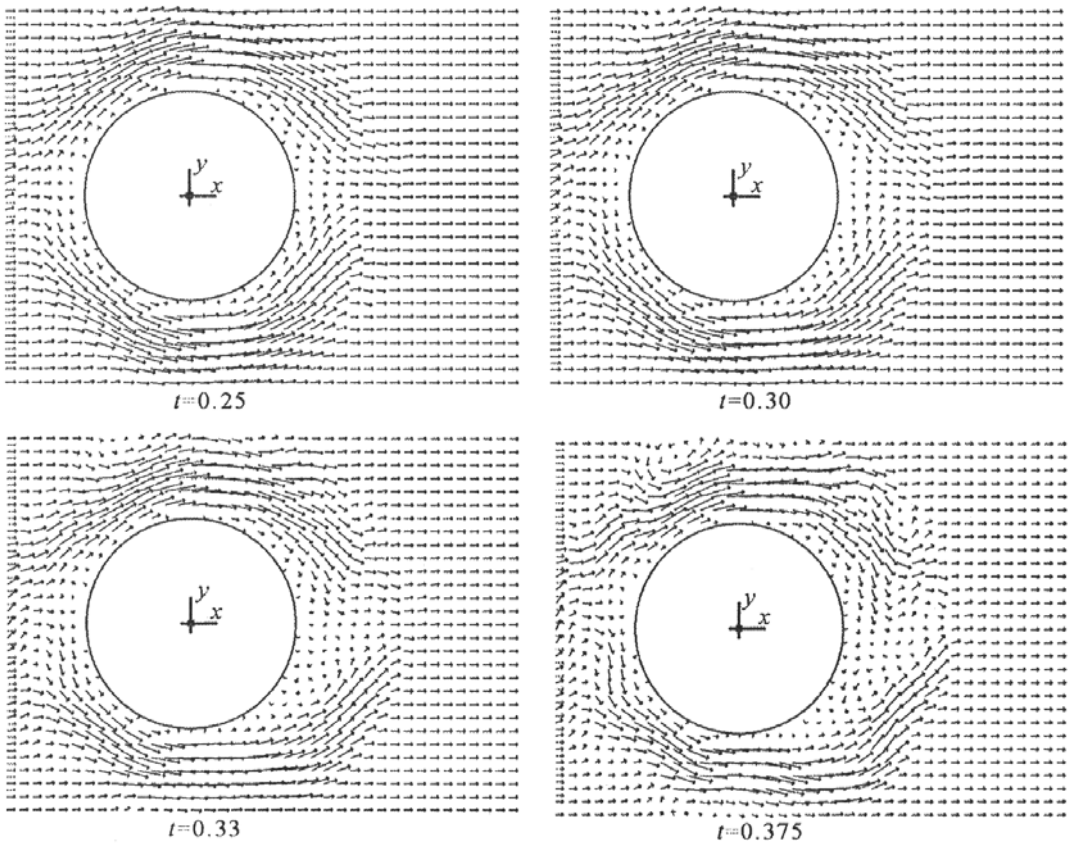

Fig. 3. Instantaneous velocity field computed for Re=200 (magnetons with the polynomial core function $g_2(r)$, Adams-Bashforth 3rd order integration scheme with $\Delta t = 0.01$)

direction of rotation. In a physically plausible velocity field, one should observe clock-wise rotating vortices shed in approximately equal time periods from the upper part of the back side of the contour, and vortices rotating in a opposite direction, shed from the bottom part of the back side of the contour. This phenomenon was not seen in the simulations. Instead, irregular vortex structures surrounding the contour and attached to it rather than flowing downstream were obtained. It turned out that the choice of the parameters of simulations (e.g. the time-integration step, the type of the core function and others) led to qualitatively similar, physically erroneous results. The use of the RK4 integration scheme gave a slightly better effect in the sense that at least the initial development of the wake (simultaneous shedding of a pair of symmetrically located, counter-rotating vortices) was re-produced. This can be seen in the upper-right picture in Fig. 4 presenting a magnification of the flow details right behind the contour.

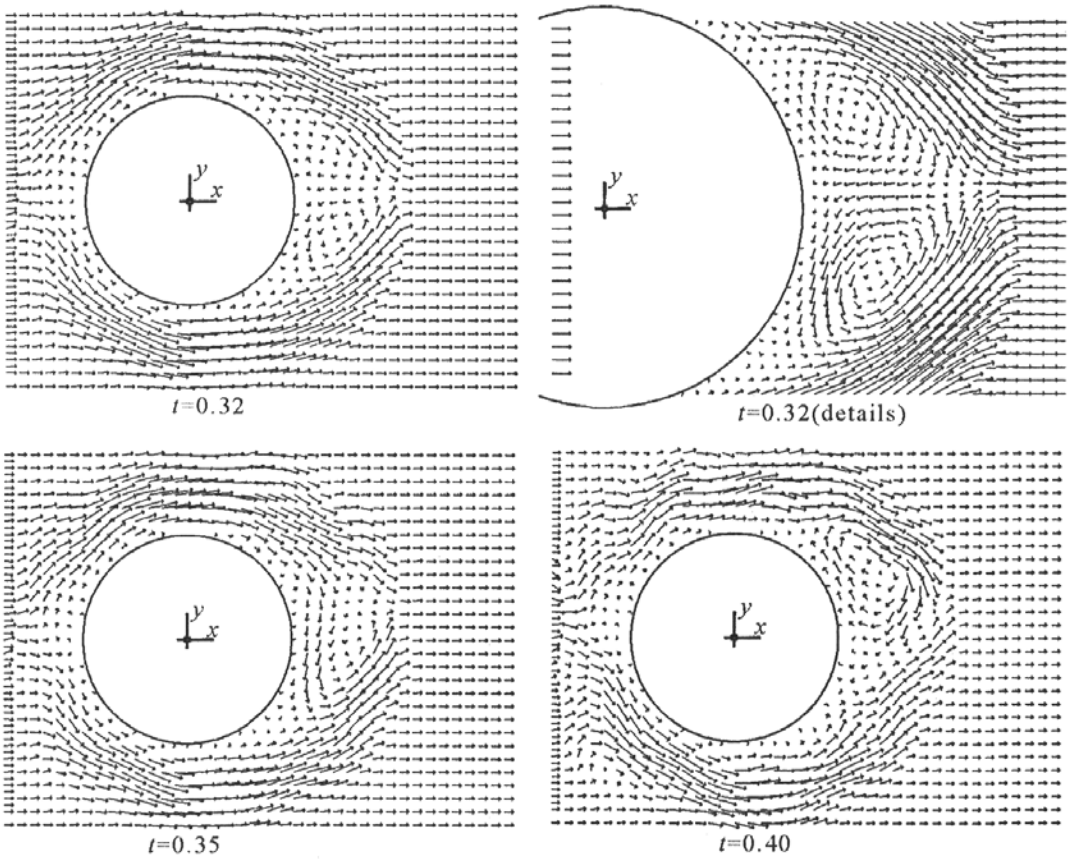

Fig. 4. Instantaneous velocity field computed for Re=200 (magnetons with the polynomial core function $g_2(r)$, Runge-Kutta 4rd order integration scheme with $\Delta t = 0.005$)

The obtained results indicate that the magnetization method (at least in the current form) is not an appropriate tool for simulating 2D flows past obstacles. Wrong results were obtained for various choices of parameters, which indicates that the source of encountered difficulties is of general nature. Since the same class of flows can be successfully computed with the use of vortex methods (see for instance Protas (2000) and references therein), the source of the problem might be the dipole character of the particles of magnetization. The particles of the vortex method are small vortex "blobs" with positive or negative vorticity distribution inside their cores. Thus, each of these particles carries a non-zero charge of vorticity (or circulation). The magnetons are quite different. Firstly, the magnetons move also due to self-induction, whereas the vortex blobs do not. Secondly, the magnetons are subject to stretching and consequently their charges are time-dependent. The vortex particles in 2D preserve their charges during motion because the equation of the vorticity

transport in 2D does not contain the stretching term. Thirdly, the magnetons are vortex dipoles, i.e. half of the magneton core is filled with positive and the other half with negative vorticity. This difference is crucial. The direct consequence of the dipole nature is that the total charge of vorticity of each magneton remains equal to zero. This is why typically a large set of overlapping magnetons will correspond to a rather oscillatory distribution of vorticity. It seems that any Lagrangian method capable of proper re-production of structures in wakes behind bluff bodies should admit spatial separation of large regions of smoothly distributed vorticity of uniform sign. The magnetization method in 2D apparently fails in this respect.

There is one more issue. In order to obtain physically meaningful results of the simulation of a flow past an obstacle using the vortex method, an additional condition should be imposed on the vorticity field. This condition appears due to the multi-connectivity of the flow domain and it ensures that the pressure field corresponding to calculated velocity and vorticity fields is a univalued function of spatial variables (see for instance Szumbarski and Styczek (1997) for further details). In the case of a flow past a single contour, the condition is equivalent to the demand that the circulation of the velocity calculated along any closed line surrounding the contour of the body and all vortex particles should be zero. An additional effect of this requirement is also the stabilization of temporal evolution of the vorticity field. Indeed, the condition means that the total charge of vorticity in the flow domain is fixed in time, i.e., unlimited generation of the vorticity of the same sign is prohibited. The natural question is whether an analogous constraint is necessary in the case of the magnetization method. Formally, the answer is negative. In the vortex method, the procedure of the pressure recovery is based on the Navier-Stokes equation, where the pressure appears under the gradient operator. This is why the integral of the rest of terms of the N-S equation, calculated along any closed path in the flow domain has to vanish. In the case of the magnetization however, the pressure is evaluated from an algebraic rather than differential problem, yielding an unambiguous solution without additional assumptions.

6.2. Simulation of a 3D flow past a spherical body

In the 3D case, the magnetization method was tested on the example of a flow past a spherical body. The objective of the computations was twofold. Firstly, the ability of the method to correctly simulate the process of vortex shedding was to be established. Secondly, the possibility of obtaining large-time, efficient simulations of the flow in a wake behind the body was to be assessed.

The results of computations presented in this paper were obtained using the finite-core magnetons with the core function $g(r) = (\frac{r}{a})^2 - \frac{8}{5}\frac{r}{a} + \frac{3}{5}$. Again, two different methods of time-integration were used: the fourth order Runge-Kutta method (RK4) and the third-order Adams-Bashforth method (AB3). The stretching was computed using the method described above, where volume integral (4.7) was transformed to a threefold iterated integral evaluated by the Gaussian quadrature.

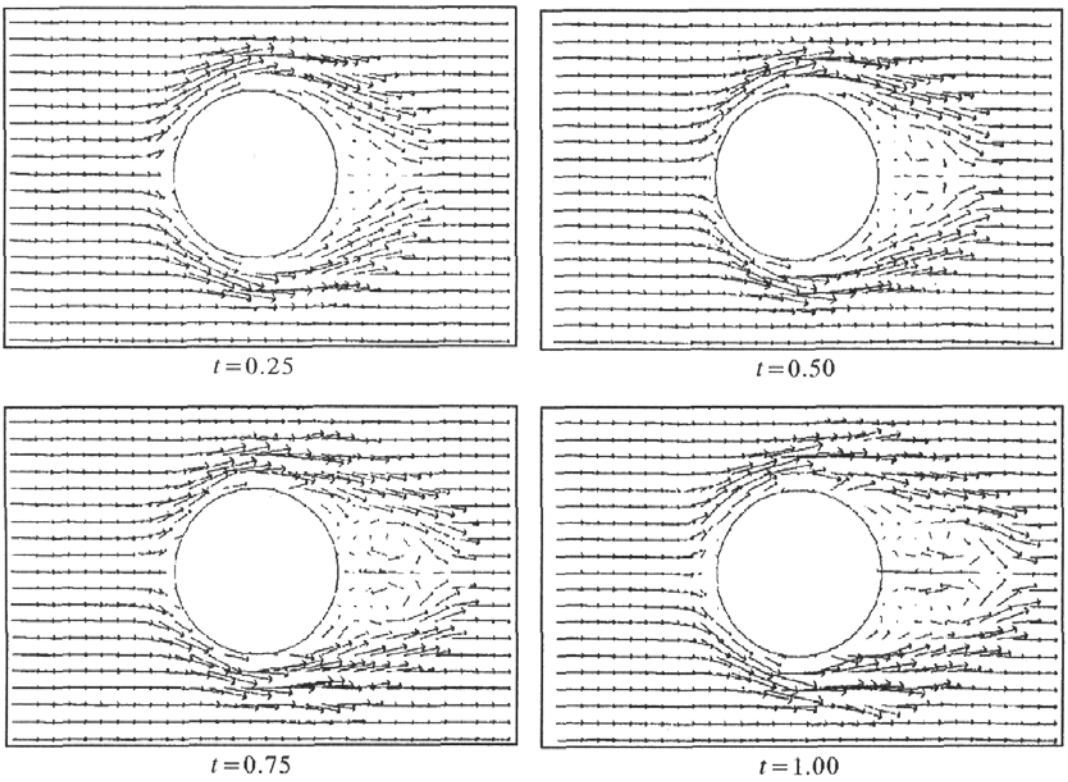

Fig. 5. Instantaneous velocity of flow past a sphere (Re=200). AB3 integration method ($\Delta t = 0.005$). The number of the magnetons created in one time step is 400

The results obtained for the Reynolds number Re=200 are presented in Fig. 5. This figure shows a time sequence of velocity projections on a plane parallel to the uniform stream at infinity and passing through the center of the sphere. The integration method is AB3 with the time step $\Delta t = 0.05$. The number of magnetons generated in each time step near the body surface is 400. One can observe the development of the first toroidal vortex structure shed from the body surface. The vortex moves away from the body and the next structure begins to form – the aerodynamic wake emerges. The streamwise extension of the wake at the time instant $t = 1$ is approximately equal to the diameter of the sphere.

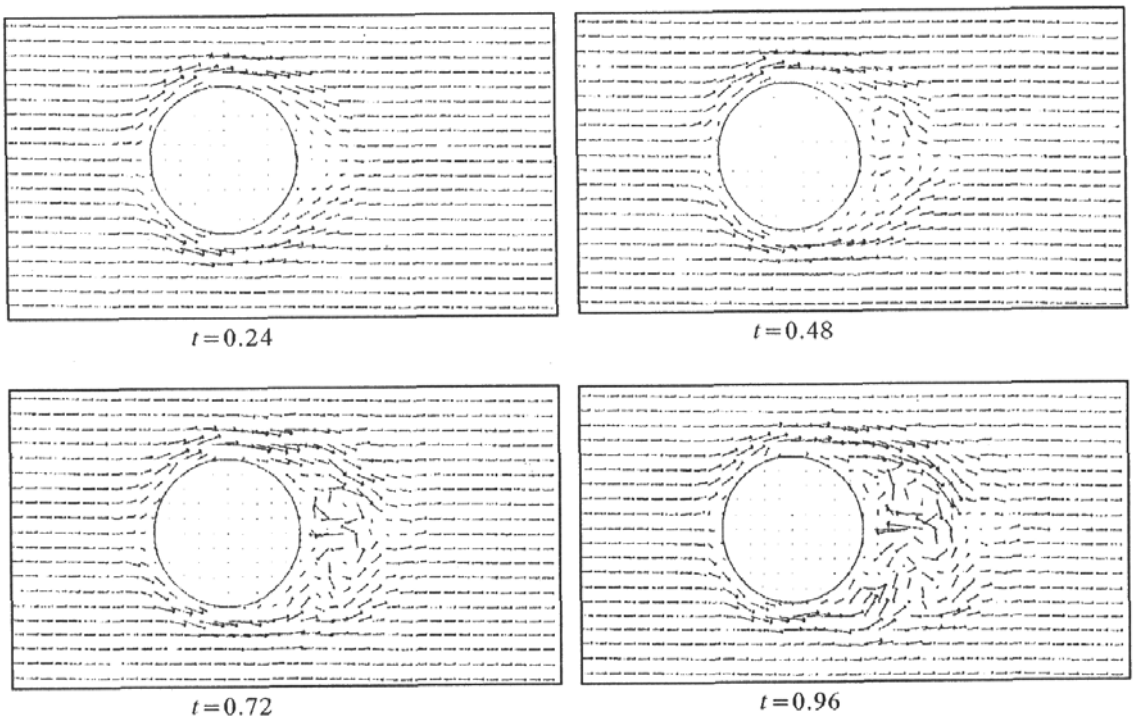

Fig. 6. Instantaneous velocity of flow past a sphere (Re=200). AB3 integration method ($\Delta t = 0.03$). The number of the magnetons created in one time step is 686

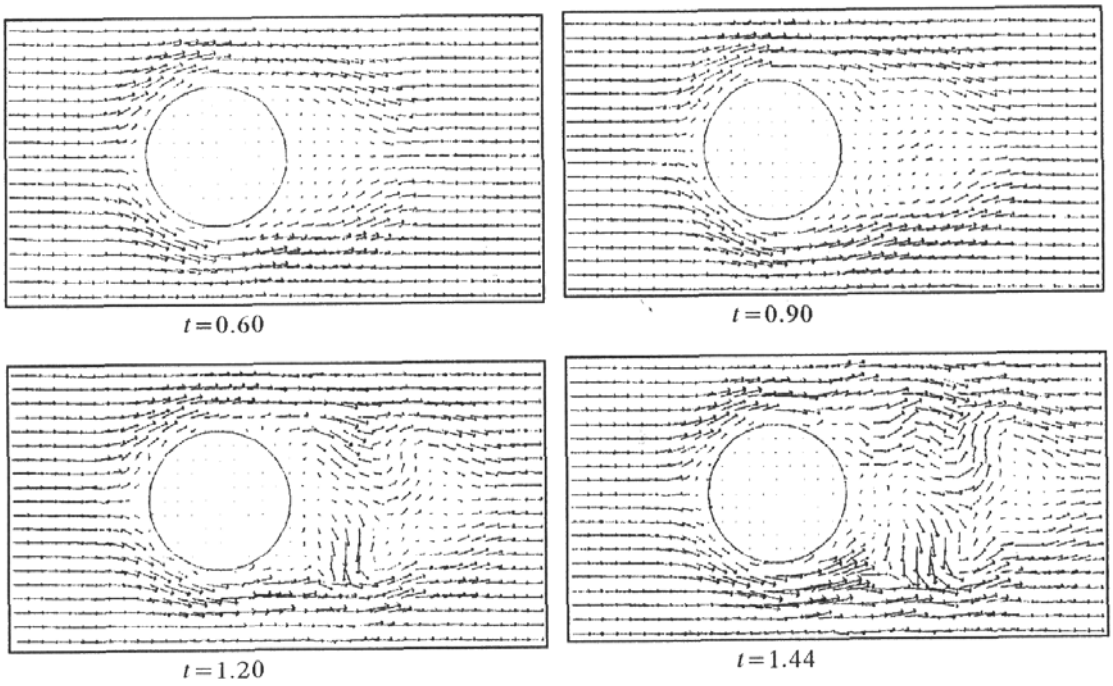

Fig. 7. Instantaneous velocity of flow past a sphere (Re=150). RK4 integration method ($\Delta t = 0.03$). The number of the magnetons created in one time step is 500

In order to enhance the resolution and improve the accuracy of the enforcement of no-slip condition at the body surface, the computations were repeated with an increased number of magnetons injected to the flow domain at each time step. Figure 6 shows instantaneous velocity patterns obtained for 686 new magnetons at each time step. The time step was reduced to $\Delta t = 0.03$. The velocity field evolved in a similar manner, and a fully developed primary toroidal vortex could be observed at $t = 0.4$. In the course of time, however, a numerical instability appeared. The wake began to loose symmetry, local values of the velocity behind the body and the charges of magnetization carried by individual magnetons tented to grow rapidly. The same effect appeared when the time-integration scheme was changed to the RK4 method. The example, computed for Re=150, is presented in Fig. 7. Initially, the development of the wake structure was physically correct. Due to a lower Reynolds number, the (approximately) symmetric vortex pattern existed for a longer time and extended farther behind the body. While the simulation was continued, the numerical instability of rapidly growing magnitude appeared, leading to "blow-up" of the local values of the velocity field.

One can suppose, that the way to avoid the instability is simply the time-step reduction. This is an idea dictated by both theory and practice of solving numerical differential problems. In the case of magnetons, the situation is, however, more complex. The point is that the number of differential equations grows quickly in time – every time step several hundreds of magnetons are being injected into the flow domain. Each additional magneton means another six differential equations in the system, so after forty-fifty steps the number of equations exceeds a hundred thousand. Larger systems of equations usually require stronger restrictions on the time-step. Eventually, the number of magnetons appearing in the flow domain during a given period increases rapidly with time. This growth can be faster when some re-meshing (or rezoning) procedure is introduced in order to maintain the degree of local overlapping of the magnetons. This is why time-consuming simulations of 3D flows in the presence of solid boundaries pose a great computational challenge. In practice, such simulations can be done successfully only when the time step is kept reasonably large. In 2D simulations with the vortex method, it is indeed the case. In a 3D case, the evolution of each magneton is described by six (instead of two) scalar values (coupled also by the stretching effect, not present in the 2D case), and "crude" time-integration can only work for a very limited time.

In spite of the failure of long-time simulations, the initial stages of the wake development are, in essence, reproduced correctly.

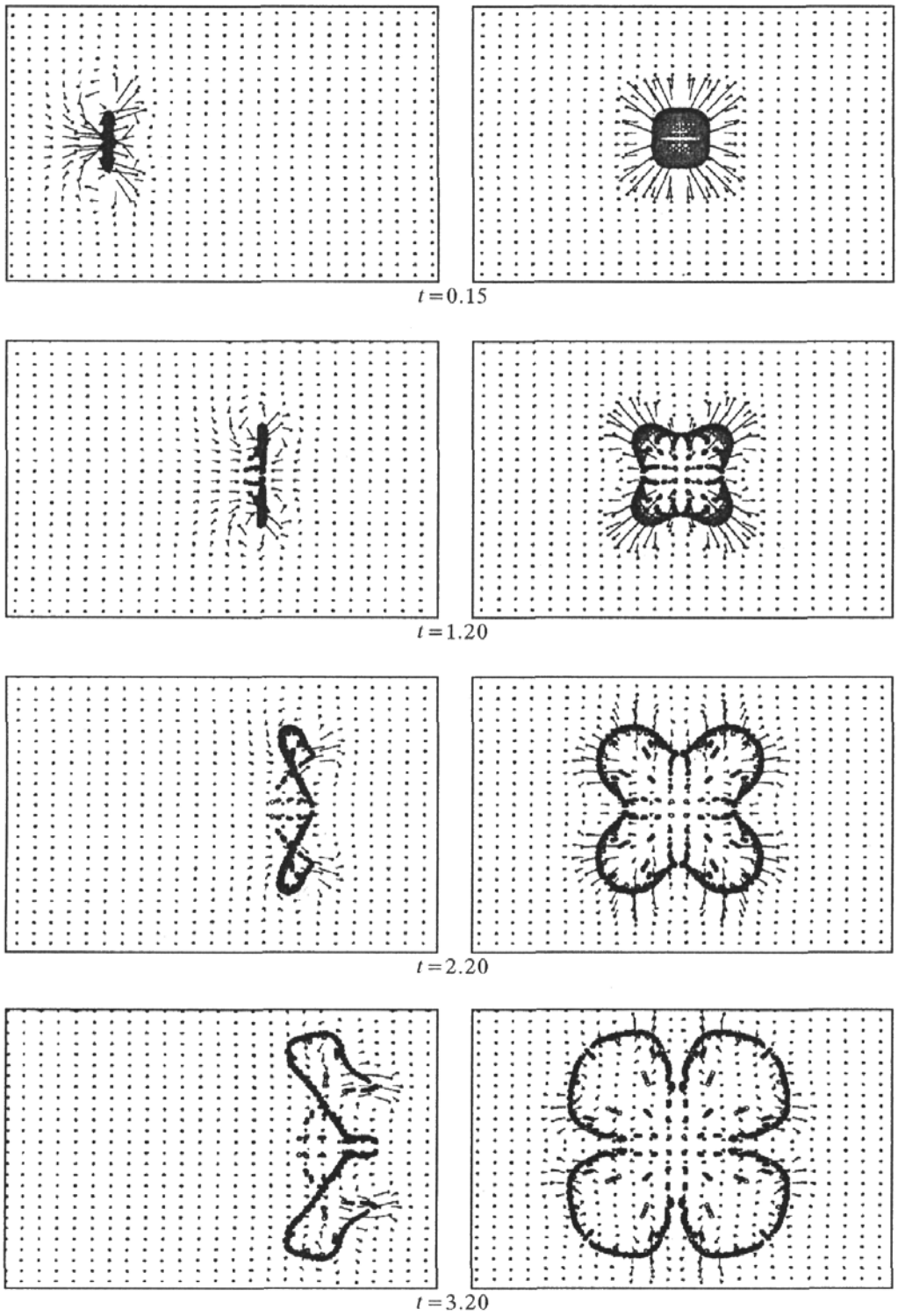

Fig. 8. Instantaneous velocity field and the positions of the magnetons computed in the simulation of the 3D vortex flow in the unbounded domain. Set text for details

6.3. Simulation of the vortex structure in an unbounded 3D space

In this section, we present an example of simulation in an unbounded 3D space. The object of the simulation was a three dimensional magnetization structure with an inviscid fluid. At the initial time instant, the structure had a form of a thin box constructed from five parallel square layers, each containing 1600 densely packed magnetons. The initial orientation of the characteristic vectors of all magnetons was perpendicular to the layers. The initial charges of the magnetons depended on the distance from the center of the structure, i.e. the "strongest" magnetons were located along the edges. The core function was exponential (cores were infinite) and the localization parameter σ was equal to 0.5. The integration scheme was RK4 with fixed time step $\Delta t = 0.001$.

Figure 8 presents obtained results. The sequence of pictures shows the evolution of the magneton locations and induced velocity field. The pictures in the left column show the side projection of the magneton central points and the projection of the velocity field on the vertical plane of symmetry. The pictures in the right column show the front projection of the magneton centers and the projection of the velocity field on the plane oriented perpendicularly and crossing the structure at approximately half of the distance between left-most and right-most magnetons. The positions of magnetons are shown with respect to the same motionless reference frame. One can see that initially the structure moves quickly, because closely packed magnetons induce collectively large velocity. Later, the movement gradually looses homogeneity and the structure starts to develop a geometrical deformation. At the same time it slows and starts to expand sideways. The remarkable feature of this expansion is that the structure preserves its original symmetry. This fact is consistent with the existence of motion invariants (see Chorin, 1994). A long-time simulation poses no problem (in contrast to the flow past an obstacle, the number of magnetons is fixed), however, later certain parts of the flow domain do not contain the sufficient number of particles to maintain appropriate spatial resolution. Thus, for serious long-time simulations some "re-meshing" strategy would be needed.

7. Final remarks and conclusion

At the first glance, the equation of the magnetization seems to be a perfect candidate for discretization with a Langrangian approach. It has a form of an advection-diffusion equation with the source term (stretching). In contrast

to the vorticity field, the magnetization is not restricted by a divergence-free condition. This means that one can define a "piece" of the magnetization, i.e. choose a small region of space and fill it with a unidirectional vector field vanishing at and outside the boundary of this region. Assuming further some symmetry properties, one arrives of the magnetization particle called the magneton.

This construction is elegant and mathematically rigorous. In does not have any counterpart for the vorticity, simply because the divergence-free vector field is *ex definitione* source-less. The induction law is obtained by well-defined mathematical operations called the Hodge projection. The procedure applied to the magneton yields an explicit, relatively simple formula.

The magnetization equation reveals some deeper structure of fluid mechanics. When the viscosity is neglected, this equation describes the dynamics of an infinite dimensional Hamiltonian system (see Chorin, 1994). Following the Lagrangian approach, one can discretize the magnetization by a set of magnetons. This way, one obtains a finite dimensional system, which inherits important properties (invariants of motion) of the continuous system.

The viscosity term appears in the equation of magnetization in the form completely analogous to the equation of vorticity. Thus, it does not introduce any additional difficulty as it can be treated in exactly the same way as in the vortex methods. The random walk can be an immediate choice, however, some higher order deterministic approaches would be feasible, too.

Finally, the stretching or source term in the equation of magnetization seems to be more tractable that the analogous term in the vorticity equations (in 3D). If the appropriate gauge transform is applied, the stretching tensor with a non-zero trace can be obtained. This means that the "filaments" of the magnetization do not have to preserve their volumes (in an inviscid motion), as do the filaments of the vorticity. This is why the magnetization-based method should be, in principle, less sensitive to resolution requirements.

In view of all advantages mentioned above, the numerical experience with the magnetization method is rather disappointing. The method turned out to be capable of simulating properly only short-time evolution of 3D flows around immersed bodies. In the two-dimensional case, the method failed even to reproduce properly the phenomenon of the vortex shedding.

It seems that the weak point of the method is its inability to spatially approximate separated 2D regions of the vorticity of a uniform sign. In the 3D case, the vorticity structure of the magnetons is not a serious obstacle because the problem of the approximation of closed vortex tubes can be solved by distributing the magnetization in the three- dimensional disk-like region

"spanned" on the tube. Certainly, such a procedure is not very "efficient", in the sense that the approximation of the "almost" one-dimensional structure in the vorticity field requires the "almost" two-dimensional distribution of the magnetization. In other words, vortex lines or tubes have to be approximated using the magnetization distributed on much larger subsets of the 3D space.

Even in the 2D case, the difficulty with the approximation can be overcome by introducing the magnetons of different sizes. Actually, the full scale of sizes should be introduced, i.e. the smallest magnetons should conform the resolution requirement, while the largest ones should be comparable to the dimension of the computational domain. This solution is however entirely inconsistent with the general idea of the Lagrangian approach which assumes that the particles used in simulation are very tiny.

Summing up it is rather not likely that the magnetization method could be competitive to vortex methods in the area of 2D flows. Like in the three-dimensional case, the question remains open. The unquestionable advantage of the method is its solid theoretical background. Further development will require the identification of the mechanism of instability described in the paper, designing efficient re-meshing algorithms as well as methods of rapid evaluation of induced velocity.

Acknowledgements

This work has been supported by the State Committee for Scientific Research (KBN), grant No. 7 T07A 022 14.

References

1. BUTTKE T.F., CHORIN A.J., 1993, Turbulence calculations in magnetization variables, *Appl. Numer. Methods*, **47**, 12
2. CHORIN A.J., 1994, *Vorticity and Turbulence*, Springer Verlag
3. GARDINER C.W., 1990, *Handbook of Stochastic Methods*, 3rd Ed. Springer Verlag
4. PROTAS B., 2000, Analysis and Control of Aerodynamic Forces in the Plane Flow past a Moving Obstacle – Application of the Vortex Method. Ph.D. Thesis. Warsaw University of Technology
5. STYCZEK A., SZUMBARSKI J., 2002, On the magnetization-based Lagrangian methods for 2D and 3D viscous flows. Part 1: Theoretical background, *Journal of Theoretical and Applied Mechanics*, **40**, 2, 339-355

6. SZUMBARSKI J., STYCZEK A., 1997, The stochastic vortex method for viscous incompressible flow in a spatially periodic domain, *Arch. Mech.*, **49**, 1, 209-232

Lagrangeowska metoda magnetyzacji dla dwu i trójwymiarowych ruchów płynu lepkiego. Część II – Realizacja numeryczna i wyniki

Streszczenie

W tej części pracy przedstawiono realizację numeryczną i opis wyników wyznaczania ruchów cieczy lepkiej uzyskanych lagrangeowską metodą cząstek magnetyzacji. Podano szczegóły wyznaczenia członu źródłowego (tzw. *stretching term*). Zaproponowano szczególny nowy sposób postępowania związany z tym efektem. Praca zawiera wyniki symulacji opływów dwu i trójwymiarowych oraz dyskusję napotkanych trudności. Podano też wyniki symulacji ewolucji swobodnych struktur wirowych. Modelowanie takich struktur jest prostsze wobec braku warunku brzegowego.

Manuscript received January 17, 2002; accepted for print May 9, 2002